

■ **CARTILAGE**

# The effectiveness of platelet-rich plasma gel on full-thickness cartilage defect repair in a rabbit model

**F. Slimi,  
W. Zribi,  
M. Trigui,  
R. Amri,  
N. Gouiaa,  
C. Abid,  
M. A. Rebai,  
T. Boudawara,  
S. Jebahi,  
H. Keskes**

From Faculty of  
Medicine, Sfax, Tunisia

**Aims**

The present study investigates the effectiveness of platelet-rich plasma (PRP) gel without adjunct to induce cartilage regeneration in large osteochondral defects in a rabbit model.

**Methods**

A bilateral osteochondral defect was created in the femoral trochlear groove of 14 New Zealand white rabbits. The right knees were filled with PRP gel and the contralateral knees remained untreated and served as control sides. Some animals were killed at week 3 and others at week 12 postoperatively. The joints were harvested and assessed by Magnetic Resonance Observation of Cartilage Repair Tissue (MOCART) MRI scoring system, and examined using the International Cartilage Repair Society (ICRS) macroscopic and ICRS histological scoring systems. Additionally, the collagen type II content was evaluated by the immunohistochemical staining.

**Results**

After 12 weeks post-surgery, the defects of the PRP group were repaired by hyaline cartilage-like tissue. However, incomplete cartilage regeneration was observed in the PRP group for three weeks. The control groups showed fibrocartilaginous or fibrous tissue, respectively, at each timepoint.

**Conclusion**

Our study proved that the use of PRP gel without any adjuncts could successfully produce a good healing response and resurface the osteochondral defect with a better quality of cartilage in a rabbit model.

**Cite this article:** *Bone Joint Res* 2021;10(3):192–202.

**Keywords:** PRP, Osteochondral, Defect, Rabbit knee, Immunohistochemical study, Histological study

**Article focus**

■ Platelet-rich plasma (PRP) may stimulate chondrogenesis and accelerate the repair of full-thickness cartilage defects in rabbits.

**Key messages**

■ The use of PRP gel results in increased chondrogenic markers expression and complete regeneration of cartilage.

**Strengths and limitations**

■ Our results indicate that the use of PRP gel without adjunct can regenerate the osteochondral full-thickness defects in the femoral condyle of a rabbit model.

- The lack of a standard method of PRP preparation and the interactions of the endogenous synthesis of PRP may remain a subject of controversy.
- The use of PRP gel without adjunct leads to good results of cartilage regeneration in an aspect of image, MRI, histology, and immunohistochemistry analysis.

**Introduction**

Articular cartilage is well known by a limited self-repair capacity due to the low cellular mitotic activity of chondrocytes and to its avascularity.<sup>1</sup> Small cartilaginous lesions may spontaneously heal; however, larger defects are expected to lead to progressive joint

Correspondence should be sent to  
Fathia Slimi; email:  
slimifathia@gmail.com

doi: 10.1302/2046-3758.103.BJR-2020-0087.R2

*Bone Joint Res* 2021;10(3):192–202.

destruction and osteoarthritis (OA),<sup>2</sup> thus making therapeutic interventions necessary.

In fact, the quality of regenerated tissue in the osteochondral defect in the knee presents a challenge for both researchers and orthopaedic surgeons. Various processes were conducted to induce the healing of large cartilage defects such as arthroscopic interventions, marrow tapping techniques, osteochondral auto-/allografting, cell-based techniques, growth factors, and emerging gene therapy techniques.<sup>3</sup> Therapeutic interventions remain unsatisfactory and the repaired tissue is usually fibrous or fibrocartilaginous, characterized by a lack of biomechanical properties.

Numerous biomaterial (natural and synthetic) additives were tried for articular cartilage tissue engineering. However, several limitations were reported, such as the incongruity between the size of transplants and the amount of cartilage that could be removed from the non-critical area of the knee, donor site morbidity, the potential risks of transmitting animal-originated pathogens, and the local pH reduction and inflammation caused by the lack of natural sites for cell adhesion.<sup>4</sup> Meanwhile, their combination has shown good results in an in vivo study.<sup>5</sup> Based on the tissue engineering approach, much attention has been paid to the bioactive agents, such as recombined growth factors, that can decrease cartilage degeneration and help the body to heal. In this annotation, the autologous blood derivatives such as purified cytokines, various matrix materials, cell-based therapy, and PRP appear to have the most potential for augmentation of tissue healing and regeneration.<sup>6</sup> As a result of these potential concerns, an alternative approach based on an autologous, biological, and safe material, combining the growth factors' advantages and the efficacy of scaffold such as PRP gel was used in the present research.

PRP is an autologous blood product derived from whole blood centrifugation and contains a high concentration of platelets. Serving as a porous bioactive scaffold for cartilage repair,<sup>7</sup> PRP gel, activated by thrombin or calcium chloride, releases several growth factors such as platelet-derived growth factor (PDGF), transforming growth factor (TGF), insulin-like growth factor (IGF), epidermal growth factor (EGF), and vascular endothelial growth factor (VEGF).<sup>8,9</sup> Numerous studies demonstrate that PRP promotes chondrocyte proliferation by increasing proteoglycan and collagen II content (in vitro),<sup>10,11</sup> leading to an increase of the quality and quantity of the cartilage repaired tissue. We presume that the PRP gel scaffold is a promising treatment for the full-thickness osteochondral defect by inducing cartilage tissue regeneration in a short experimental time.

The objective of our study was to evaluate the effects of PRP gel used as an alternative treatment for a full-thickness cartilage defect in a rabbit model.

**Table 1.** International Cartilage Repair Society macroscopic cartilage repair assessment.

Cartilage repair assessment ICRS	Points
<b>Degree of defect repair</b>	
In level with surrounding cartilage	4
75% repair of defect depth	3
50% repair of defect depth	2
25% repair of defect depth	1
0% repair of defect depth	0
<b>Integration to border zone</b>	
Complete integration with surrounding cartilage	4
Demarcating border < 1 mm	3
3/4 of graft integrated, 1/4 with a notable border > 1 mm width	2
1/2 of graft integrated with surrounding cartilage, 1/2 with a notable border > 1 mm	1
From no contact to 1/4 of graft integrated	0
<b>Macroscopic appearance</b>	
Intact smooth surface	4
Fibrillated surface	3
Small, scattered fissures or cracks	2
Several small or few but large fissures	1
Total degeneration of grafted area	0
<b>Overall repair assessment, number of points</b>	
Grade I: normal	12
Grade II: nearly normal	11 to 8
Grade III: abnormal	7 to 4
Grade IV: severely abnormal	3 to 1

ICRS, International Cartilage Repair Society.

## Methods

**Animals.** All surgical procedures and care for rabbits were approved by the Animal Research Ethics Committee of our university, in compliance with the internationally recognized principles for the care and use of laboratory animals, and judged commendable by the Committee of Animal Ethics (Protocol no. 94–1939). An ARRIVE checklist has been provided in the Supplementary Material to show that the correct protocol has been followed. A total of 14 New Zealand white rabbits, weighing between 2.5 and 3 kg, and with a mean age of seven months (6.5 to 7.5), were used in this study. An osteochondral rabbit model was used for this study as the knee is large enough and easy to manipulate. For all animals, the right knee was treated with PRP and the left knee remained untreated. Each rabbit served as its own control. All rabbits were fed on a standard diet and kept in individual cages, allowing free activity during the experimental procedure. Seven rabbits each were killed at three and twelve weeks postoperatively.

**Preparation of PRP.** The preparation of PRP was performed simultaneously during the surgical procedures. All animals received an intramuscular administration of Ketamine (50 mg/ml; Panpharma, France) and Unicaine 2% (100 mg/5 ml; Unimed, Tunisia). After induction of anaesthesia, 10 ml of blood was collected from the lateral saphenous vein and mixed with Citrate Dextrose Acid A solution (ACD-A) to avoid coagulation; the mixing rate

**Table II.** 3D Magnetic Resonance Observation of Cartilage Repair Tissue scoring system adapted for the evaluation of ex vivo osteochondral samples.

3D MOCART score	
Category	Points
<b>Defect fill, %</b>	
0	0
0 to 25	3
25 to 50	5
50 to 75	10
75 to 100	15
100	20
100 to 125	15
125 to 150	7
150 to 200	3
> 200	0
<b>Cartilage interface</b>	
Complete	10
Demarcating border	8
Defect visible < 50%	3
Defect visible > 50%	0
<b>Bone interface</b>	
Bone interface complete	10
Partial delamination	5
Complete delamination	0
Delamination of periosteal flap	10
<b>Surface</b>	
Intact	5
Damaged < 50% depth	0
Damaged > 50% depth	10
<b>Structure</b>	
Homogeneous	5
Inhomogeneous	2
Cleft formation	0
Absence of repair tissue	10
<b>Signal intensity</b>	
Normal (identical to adjacent cartilage)	5
Nearly normal (slight areas of signal alteration)	0
Abnormal (large areas of signal alteration)	5
<b>Chondral osteophytes</b>	
Absent	3
< 50% of chondral thickness	0
> 50% of chondral thickness	10
<b>Integrity of subchondral bone plate, %</b>	
> 75	8
50 to 75	5
25 to 50	3
0 to 25	0
<b>Subarticular spongiosa</b>	
Intact	10
Granulation tissue	8
Sclerosis	8
Cyst	5
Granulation tissue and sclerosis	5
Granulation tissue and cyst	2
Sclerosis and cyst	2
Granulation tissue, sclerosis, and cyst	0
<b>Adhesions</b>	
Absent	3

Continued

**Table II.** Continued

3D MOCART score	
Category	Points
Present	0
<b>Effusion</b>	
Absent	2
Present	0
<b>Total points</b>	100

MOCART, Magnetic Resonance Observation of Cartilage Repair Tissue.

was 9:1 in volume. Furthermore, 1 ml of blood was reserved for determination of blood cells' concentration while the remainder was retained for PRP preparation procedure.

According to the protocol of PRP preparation followed by Fukaya and Ito,<sup>12</sup> the remaining blood (9 ml) was immediately centrifuged for 3,000 rpm × three minutes by the centrifuge system (EBA 20, Hettich Lab Technology) to separate the red blood cells from plasma. The plasma was then pipetted and centrifuged again at 4,000 rpm for 15 minutes. The resulting material consisted of three layers. The supernatant was discarded, the medium was the PRP, and a lower fraction of cells was mixed and carefully removed into a sterile vacurette. Next, 1 ml was kept for cytological analysis and the remaining 1 ml of PRP was transformed into gel with the addition of 10% calcium chloride (CaCl<sub>2</sub>), with ratio 0.1 ml CaCl<sub>2</sub>:1 ml PRP, and reserved for surgical use. PRP gel adhered easily to the lesion.<sup>13,14</sup>

**Experimental design.** Following anaesthesia induction, an osteochondral defect was created in the rabbits' knees. Both lower limbs were shaved and trimmed with sterile solution prior to surgical intervention. A medial parapatellar incision, involving the skin and the subcutaneous tissue, was created in each knee to expose the femoral trochlea. In the middle of the trochlear groove, an osteochondral lesion, 4 mm in diameter and 3 mm in depth, was created using a drill with perforated wick.

The defect was carefully debrided of any residues with a saline solution. Both knees were subjected to an identical surgical procedure; the left defect was not treated whereas the right defect was filled with the PRP gel prepared immediately beforehand. Thus, each rabbit served as its own control. Finally, the wound was closed using simple interrupted sutures with 4–0 resorbable sutures (Ethilon; Ethicon, Germany), and a slight compression bandage was applied. Postoperatively, all rabbits were kept in individual free cage activity; no complications were noted during the experiment.

Upon sacrifice, both knee joints were removed, identified, and placed in separate containers. Then all specimens were immediately subjected to macroscopic and MRI examinations.

**Macroscopic evaluation.** The macroscopic evaluation of all samples was performed by a blinded pathologist (NG)

**Table III.** International Cartilage Repair Society visual histological assessment scale.

Feature	Points
<b>I. Surface</b>	
Smooth/continuous	3
Discontinuities/irregularities	0
<b>II. Matrix</b>	
Hyaline	3
Mixture: hyaline/fibrocartilage	2
Fibrocartilage	1
Fibrous tissue	0
<b>III. Cell distribution</b>	
Columnar	3
Mixed/columnar-clusters	2
Clusters	1
Individual cells/disorganized	0
<b>IV. Cell population viability</b>	
Predominantly viable	3
Partially viable	1
< 10% viable	0
<b>V. Subchondral bone</b>	
Normal	3
Increased remodelling	2
Bone necrosis/granulation tissue	1
Detached/fracture/callus at base	0
<b>VI. Cartilage mineralization (calcified cartilage)</b>	
Normal	3
Abnormal/inappropriate location	0
<b>Safranin O stain</b>	
Normal	4
Slight reduction	3
Moderate reduction	2
Severe reduction	1
No staining	0
<b>Safranin O in defect, %</b>	
75 to 100	4
50 to 75	3
25 to 50	2
0 to 25	1
No safranin O staining	0

ICRS, International Cartilage Repair Society.

according to the International Cartilage Repair Society (ICRS) macroscopic scoring assessment scale for cartilage repair (scale of 0 to 12, with 12 being normal cartilage and 0 indicating severely abnormal cartilage; Table I).<sup>15</sup>

**MRI evaluation.** MRI is the gold standard method for noninvasive assessment of joint cartilage, providing information on the structure, morphology, and molecular composition of this tissue.<sup>16</sup> For morphologic evaluation, previously prepared specimens of medial femoral condyles were placed into an opaque box filled with ultrasound gel used in our protocol, and MRI was performed on a 1, 5 Tesla clinical imaging system (Siemens Munich, Germany). A personalized knee protocol was performed for all samples, using a cartilage-sensitive fast spin echo sequence in the sagittal plane. The samples were acquired

with a repetition time of 35 ms, an echo time of 19 ms (effective), a field of view (Fov) of 121\*148, and an acquisition time (TA) of 3.54. The matrix was 310\*5121. The MRI evaluation was performed by two blinded orthopaedists (MT and MAR) according to the MRI Magnetic Resonance Observation of Cartilage Repair Tissue (MOCART) scoring system for all specimens (Table II).<sup>17</sup>

**Cytological analysis.** Both the whole blood and PRP aliquots (1 ml) underwent cytological analysis by the automated haematology analyzer (Sysmex XP-300, Medibio Instruments, Tunisia) to determine platelet, red blood cell, and white blood cell counts.

**Haematoxylin and eosin evaluation.** All cartilage specimens were immediately fixed in buffered formalin 10% for three days. Then, they were decalcified for seven days before being embedded into paraffin. The sections were cut into 5 µm. The same position was standardized to ensure a representative view and comparability of all specimens. All sections of each group were stained with haematoxylin and eosin to evaluate the morphology of tissue. The sections were examined below different magnifications with an Eclipse 80i light microscope (Nikon, Japan).

**Safranin O assay.** Safranin O staining was used to estimate the proteoglycan content in normal cartilage. All blades were dewaxed with xylene and rehydrated with alcohol. These steps lasted, respectively, ten minutes with the Weigert's haematoxylin working solution (Biopole, Tunisia) followed by Fast green (FCF) solution (five minutes), acetic acid solution (ten seconds), and Safranin O solution (five minutes). All solutions were prepared in advance. Finally, sections were dehydrated and mounted with resinous mounting media.<sup>18</sup> All slides were evaluated and scored by two blinded pathologists (NG and TB) according to the ICRS recommendation of cartilage repair,<sup>19,20</sup> supplemented with the Safranin O staining assessment (Table III),<sup>21</sup> and imaged using a DXM 1200 C CCD camera (Nikon).

**Immunohistochemical evaluation.** The immunohistochemistry process was followed to estimate the collagen II content. The sections were clipped into 0.3 µm, then dewaxed in xylene, rehydrated, and submitted to antigen retrieval (pH 8.0). The slides were blocked for endogenous peroxidase activity through incubation in 3% H<sub>2</sub>O<sub>2</sub> for five minutes. Afterwards, they were incubated with primary mouse monoclonal collagen II antibody (5B2.5) for one hour. The secondary antibody, Anti-mouse IgG biotinylated (Vector Laboratories, USA), was used for 20 minutes. The slides were treated with the revealer diaminobenzidine (DAB) to visualize the peroxidase activity and then counterstained with haematoxylin and mounted.

**Statistical analysis.** The statistical analysis of the data was performed using SPSS statistical software (version 17.0; SPSS, USA) taking p < 0.05 as significant. Outcome variables of macroscopic and histological ICRS score and MRI MOCART score were evaluated using a non-parametric Wilcoxon signed-rank test. Cell blood counts

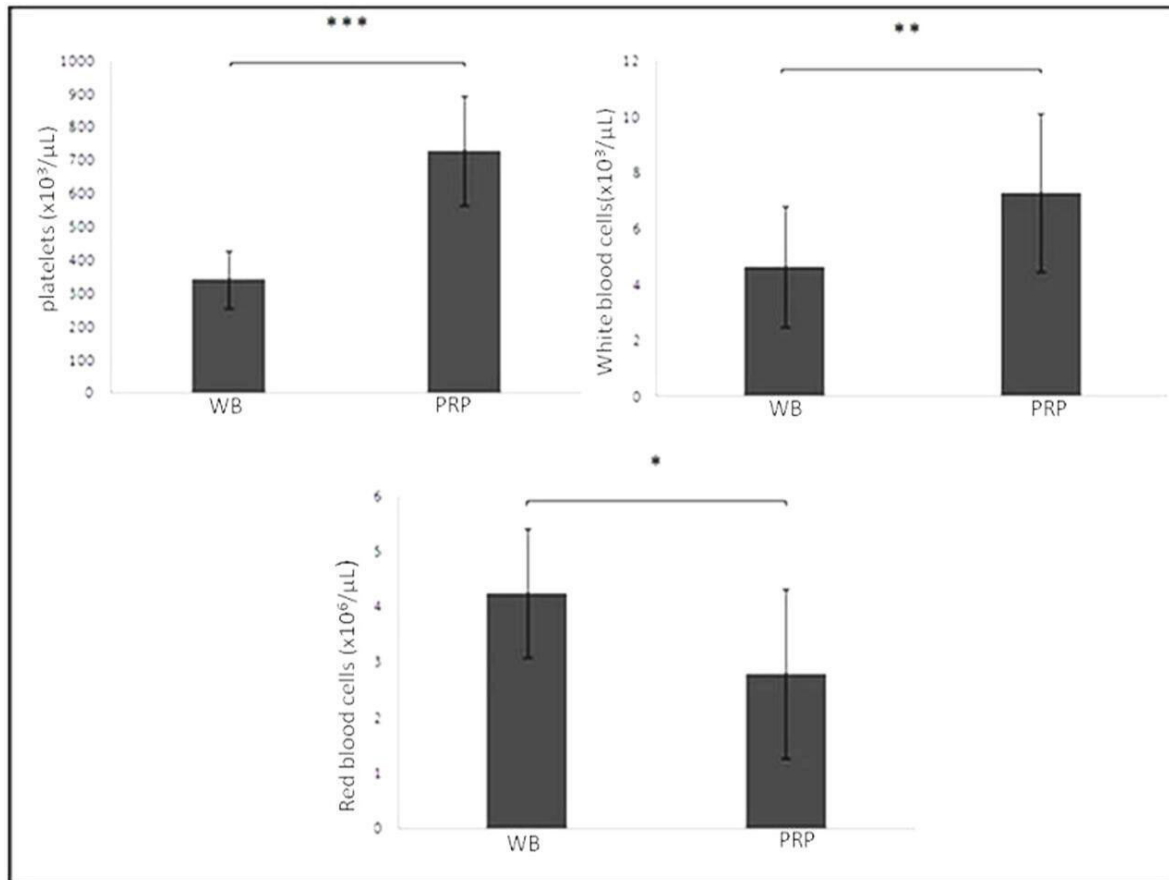


Fig. 1

Cytological analysis of the whole blood (WB) and the platelet-rich plasma (PRP) component (platelets, white blood cells, and red blood cells). All results were presented as the mean and standard deviation (SD); statistical analysis was performed to compare platelet ( $p < 0.001$ ), white blood cell ( $p = 0.007$ ), and red blood cell ( $p < 0.001$ , all non-parametric Mann-Whitney U test) concentrations in the whole blood and PRP. \* $p < 0.001$ . \*\* $p < 0.01$ . \*\*\* $p < 0.05$ .

(platelets, white blood cells, and red blood cells) were evaluated using a non-parametric Mann-Whitney U test. Results are expressed as the mean and standard deviation (SD). The correlation coefficients were calculated using a parametric correlation Pearson test to assess the interobserver reliability.

## Results

**Experimental animal observation.** All rabbits showed a healthy appearance, i.e. no signs of infection or synovitis were observed at any time during the experiment.

**Cytological assessment.** The mean platelet count of PRP ( $726.71 \times 10^3/\mu\text{L}$  (SD 164.94)) was significantly (2.13-fold) greater than that of whole blood ( $340 \times 10^3/\mu\text{L}$  (SD 85.62)) ( $p < 0.001$ , non-parametric Mann-Whitney U test). The mean white blood cell count ( $7.29 \times 10^3/\mu\text{L}$  (SD 2.83)) was higher in PRP in comparison with whole blood ( $4.63 \times 10^3/\mu\text{L}$  (SD 2.17)) ( $p = 0.007$ , non-parametric Mann-Whitney U test). In contrast, the mean red blood cell count ( $4.24 \times 10^6/\mu\text{L}$  (SD 1.16)) was higher in whole blood in comparison with PRP ( $2.79 \times 10^6/\mu\text{L}$  (SD 1.52)) ( $p = 0.015$ , non-parametric Mann-Whitney U test) (Figure 1).

**Macroscopic examination.** At week 3 after surgery, the regenerated tissue in the PRP group defect appeared glossy, translucent, and mostly well-integrated. However, the surface was not as smooth as the native articular surface. The area of the repair tissue presented the same thickness in comparison with the adjacent cartilage, with some light concavity (Figure 2b). The majority of the defects in the control group remained empty or sometimes covered with a thin brown layer (Figure 2a).

At week 12, the PRP group defect was totally filled with an opaque white tissue (around 100% repair of defect depth) with a total discernible integrity pertaining to the native cartilage. The regenerated tissue had the same aspects as the adjacent tissue. No distinguishable margin was detected (Figure 2d). In the control group, the defects were partially concave and moderately filled with a neoformed tissue, suggesting the formation of cartilage-like tissue (Figure 2c).

Macroscopic scoring analysis revealed a significant difference between treated and control groups at week 3 ( $p = 0.016$ , non-parametric Wilcoxon signed-rank test). Additionally, we observed a significant difference



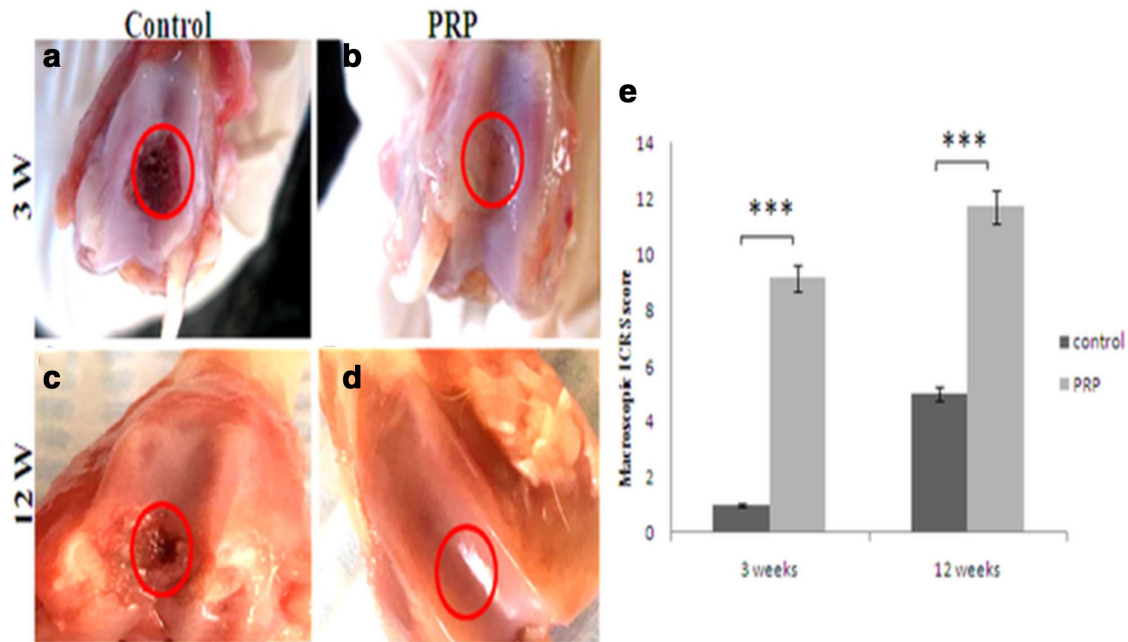


Fig. 2

Representative photographs of gross appearance of defect in trochlear groove (4 mm in diameter) at: a) and b) week 3; c) and d) week 12. a) and c) controls; b) complete restoration of the articular surface of the defect; d) similar appearance to the normal cartilage. The red circles indicate the original defect margin. e) Macroscopic assessment of cartilage repair was assessed by International Cartilage Repair Society (ICRS) macroscopic evaluation scale. Results are presented as the mean and standard deviation (SD); statistical analysis was performed to compare scores of treated and control groups. \*\*\* $p < 0.05$ , non-parametric Wilcoxon signed-rank test. Control, untreated group; platelet-rich plasma (PRP), group treated with PRP.

**Table IV.** International Cartilage Repair Society macroscopic scores at three and 12 weeks after surgery.

Variable	3 weeks			12 weeks		
	Control	PRP	p-value*	Control	PRP	p-value*
Mean degree of defect repair (SD)	0 (0)	3.43 (0.53)	0.015	1.71 (0.488)	4 (0)	0.014
Mean integration to border zone (SD)	0 (0)	2.86 (0.37)	0.011	1.14 (0.378)	4 (0)	0.014
Mean macroscopic appearance (SD)	1 (0)	2.86 (0.69)	0.016	2.14 (0.378)	3.71 (0.48)	0.015
Mean total score (SD)	1 (0)	9.43 (0.78)	0.016	5.14 (0.69)	11.71 (0.48)	0.016

\*Non-parametric Wilcoxon signed-rank test.  
PRP, platelet-rich plasma; SD, standard deviation.

between treated and control groups at week 12 ( $p = 0.016$ , non-parametric Wilcoxon signed-rank test) (Figure 2e, Table IV).

**MRI assessment.** According to the MOCART scoring system, the difference between treated and untreated groups was significant at week 3 (72.29 (SD 2.92) vs 3 (SD 0);  $p = 0.014$ , non-parametric Wilcoxon signed-rank test) and at week 12 (98 (SD 1.15) vs 5.71 (SD 1.11);  $p = 0.018$ , non-parametric Wilcoxon signed-rank test) (Figure 3e). Repair area surfaces of treated groups were regular (Figures 3b and d). On the other hand, irregular surface and inhomogeneous signal of the repaired tissue were shown in the control groups (Figures 3a and c).

**Histological findings and immunohistochemical staining for collagen II.** Haematoxylin and eosin (H&E) staining revealed that, three weeks after surgery, the defects in the control group were filled with fibrous tissue (Figure 4a).

In the PRP group, the articular surface was partially filled with incomplete cartilage regenerated tissue with a low number of cells. The morphological aspect of chondrocytes and matrix was similar to the cartilage-like tissue (Figure 4b).

At week 12, the joint surface in the control group was slightly concave and the defects were filled with fibrocartilaginous tissue with extensive chondrocyte clustering (Figure 4c). The defects in the PRP group were fully filled with hyaline cartilage-like tissue. A normal or a slight hypocellularity was shown in the repaired tissue as well as the maintenance of hyaline cartilage (Figure 4d).

The safranin O staining showed, at week 3 post-surgery, a poor or slight metachromasia in the control and PRP groups, respectively, accounting for the low expression of proteoglycan content (Figures 5a and b). At week 12, a few cartilage matrices were observed in

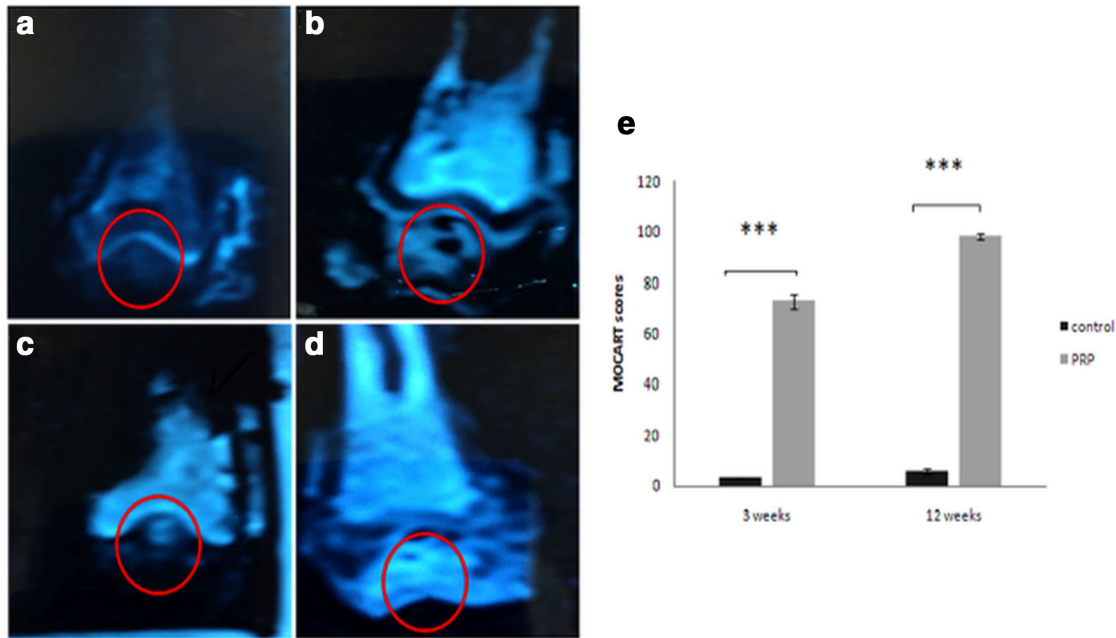


Fig. 3

Sagittal cartilage sensitive fast-spin-echo MRIs at: a) and b) week 3; c) and d) week 12. a) and c) are the control group; b) and d) were treated with platelet-rich plasma (PRP). e) The morphological MRI evaluation of cartilage repair was assessed by the Magnetic Resonance Observation of Cartilage Repair Tissue (MOCART) scoring system.<sup>17</sup> Results are presented as the mean and standard deviation (SD); statistical analysis was performed to compare scores of treated and control groups. \* $p < 0.05$ , non-parametric Wilcoxon signed-rank test. Control, untreated group; PRP, group treated with PRP.

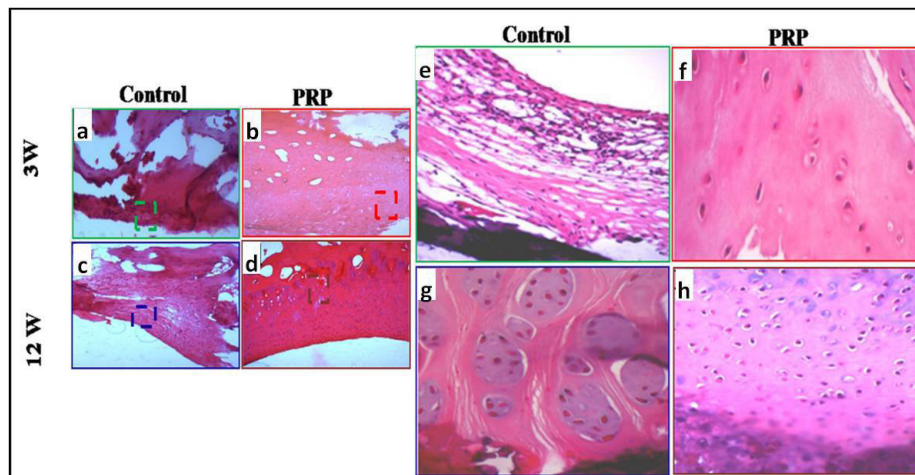


Fig. 4

a) to d) Haematoxylin and eosin staining: a) to d) original magnification: 100 $\times$ ; e) to h) original magnification: 200 $\times$ . e) and f) Microphotographs showing the repair tissue at week 3. a) and e) Control: fibrous tissue. b) and f) Presence of slightly differentiated cartilaginous tissue. c) and g) Control: fibrocartilaginous tissue. d) and h) good differentiated cartilaginous tissue at week 12. PRP, platelet-rich plasma.

the control group (Figure 5c). On the other hand, the neoformed tissue was densely stained by safranin O in the PRP group. It is similar to that of the normal hyaline cartilage, standing for high proteoglycan content (Figure 5d). The control groups displayed poor proteoglycan content in comparison to the treated groups.

The mean ICRS histological scores of PRP groups, at weeks 3 and 12 postoperatively, were higher than those of the control groups (week 3: 19.43 (SD 1.27) vs 1 (SD 0);  $p = 0.017$ , non-parametric Wilcoxon signed-rank test);

week 12: 25.43 (SD 0.53) vs 3.71 (SD 1.25);  $p = 0.016$ , non-parametric Wilcoxon signed-rank test), respectively) (Figure 6).

ICRS scoring of macroscopic and histological evaluation of cartilage repair indicated that the scores in the PRP groups were higher than those in the control groups at weeks 3 and 12.

All correlation coefficients between the ICRS macroscopic score, ICRS histological score, and MOCART score

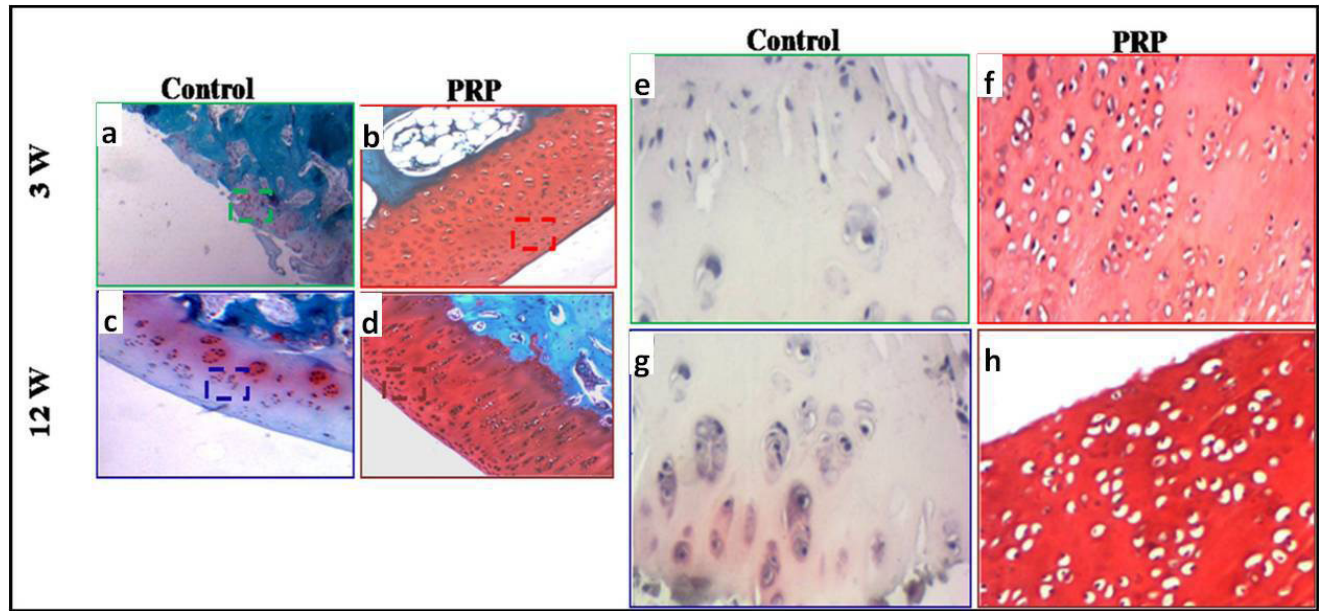


Fig. 5

Safranin O staining: a) to d) original magnification: 100x; e) to h) original magnification: 200x. Microphotographs of Safranin O/Fast green staining at: a), b), e), and f) week 3; c), d), g), and h) week 12. a), c), e), and g) control: the tissue filling the defect, showing fibrous and fibrocartilaginous tissue; b) and f) very low Safranin O staining intensity; d) and h) the cellular morphology showed round and oval cells within lacunae surrounded by an extracellular matrix, presenting an intense safranin O staining, which accounts for the high content of proteoglycan.

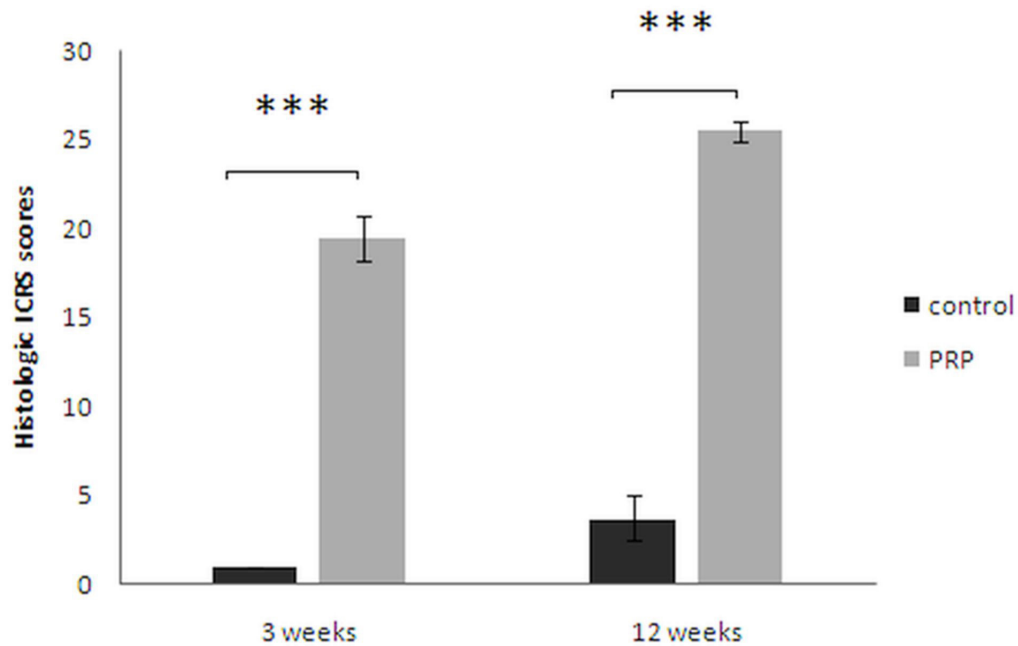


Fig. 6

Histological International Cartilage Repair Society (ICRS) scores: Haematoxylin and eosin (H&E) staining sections were evaluated according to ICRS.<sup>19,20</sup> Safranin O staining was scored as described previously by Wayne et al.<sup>21</sup> Results were presented as the mean and standard deviation (SD) in each group. \*\*\* $p < 0.05$ , non-parametric Wilcoxon signed-rank test. Control, untreated group; platelet-rich plasma (PRP), group treated with PRP.

of the treated groups were significantly high and positive with  $p < 0.001$ .

At week 12, immunohistochemical staining was dense with respect to the matrix and the chondrocytes of the PRP group (Figure 7d). The staining intensity at week 3,

however, was considerably lower (Figure 7b). The control groups showed a lack of immunohistochemical intensity staining, ascribed to the lack of collagen II expression (Figures 7a and c).



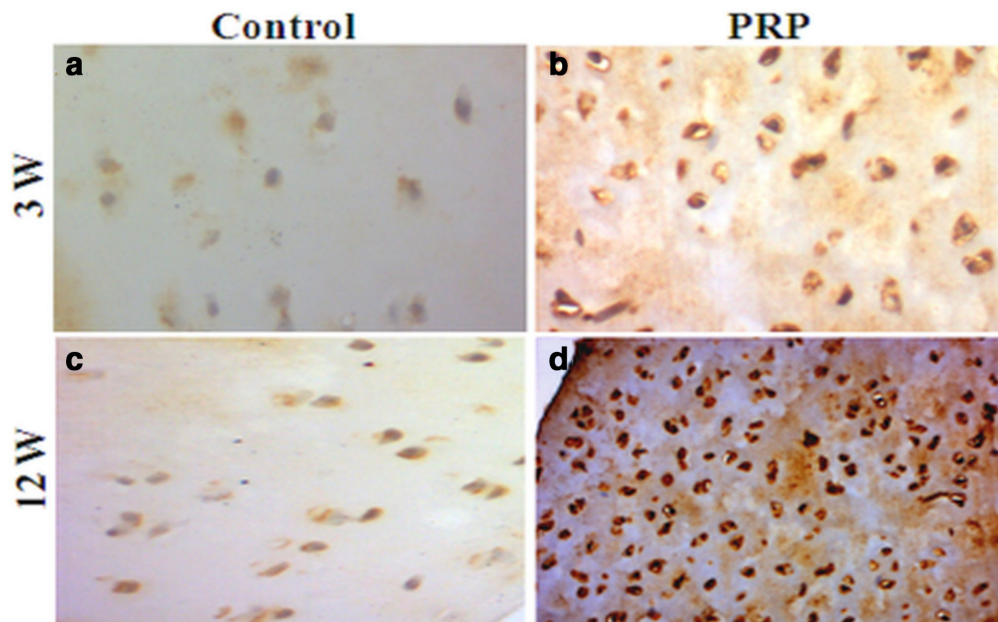


Fig. 7

Photomicrograph showing immunohistochemical staining for type II collagen at: a) and b) week 3; c) and d) week 12. a) and c) control absence of collagen II expression; b) very low amount of collagen II; d) considerable amount of collagen II. Original magnification: 200 $\times$ . PRP, platelet-rich plasma.

## Discussion

The treatment of osteochondral defects pertaining to articulating joints, namely the knee, represents a challenge in orthopaedic surgery. PRP has become an appealing alternative treatment for damaged cartilage, either traumatic or arthritic. Recent literature has shown that PRP may be helpful both as a therapeutic tool by intra-articular injection in patients affected by OA, and as an adjuvant for surgical treatment of cartilage defects.<sup>22</sup> PRP provides a local environment for tissue regeneration, due to its intrinsic regenerative properties (growth factors).<sup>23</sup>

A range of PRP preparations have been reported, including activated PRP, PRP releasate, PRP gels, and nonactivated PRP liquid.<sup>24</sup> However, PRP gel bioscaffolding may be the adequate form to investigate in our study. This form acts as a 3D template for cellular propagation and growth factors seeding, as shown by its random mesh-like structure with cross-linked fibrin<sup>25</sup> and its adhesive properties.<sup>26</sup> Contrarily to the injected soluble PRP form where most growth factors undergo rapid dispersion,<sup>1</sup> PRP gel fills the created defect, and the growth factors are released as the fibrin biodegrades.

To our knowledge, few studies have used PRP gel as a primary management strategy without any adjuncts or scaffolding in a rabbit model. Our study constitutes a sound model of this concept. Depending on how PRP is generated, the present PRP preparation method provided an intermediate platelet concentration (2.13-fold) that was more effective than low concentrations (suboptimal) and high concentrations (inhibitory effect).<sup>27</sup> In addition, the low leucocyte concentration was shown to be coordinated, and cooperative activities were reported between

platelets and all components of whole blood, especially the leucocytes. Acute inflammation could be limited and tissue repair was triggered in the wound healing process.<sup>28</sup>

In our study, a critical-sized cartilage defect (4 mm in diameter and 3 mm in depth) was selected, due to the difficulty of spontaneous repair of a large defect (> 3 mm in diameter),<sup>29,30</sup> to evaluate the regenerative potential of PRP gel. The defect reached the subchondral bone, causing some bleeding. PRP constitutes an adequate means for increasing the platelet concentration inside the injured tissues and enhances the quantity and the quality of tissue repair.<sup>13</sup>

Our findings exhibited a low amount of neoformed tissue in the untreated knees at weeks 3 and 12; in contrary to the defects treated with PRP gel that displayed a partial degree of regenerative tissue at week 3 and a complete restoration at week 12, exhibiting a smooth articular surface. In comparison with the study of Xie et al,<sup>7</sup> our findings showed better cartilage regeneration in a shorter experimental time. There was a statistically significant difference between the treated and the control groups. The results were in accordance with the previous studies that evaluated the PRP capability to induce the complete cartilage restoration in an osteochondral sheep model.<sup>26</sup>

The MRI morphological findings, performed via the MOCART scoring system, confirmed the macroscopic results showing a considerable structural difference in terms of defect fill of the PRP group compared to controls.

The histological analysis of the untreated groups exhibited a neoformed fibrous or fibrocartilaginous tissue. This spontaneous regeneration might be ascribed

to the recruitment of mesenchymal cells derived from the subchondral bone bleeding base in the defects. This tissue has no similarity with the normal cartilage properties and tends to deteriorate quickly when submitted to repetitive weight-bearing.<sup>31,32</sup> The slight metachromasia and low expression of COL II results may prove a deficient matrix with lower proteoglycan content for PRP-treated knees at three weeks; although this deficiency could be ameliorated over time (12 weeks) with high matrix and chondrocyte production. Abundant proteoglycan content and high expression of COL II indicated hyaline cartilage regeneration. The treatment of the defects with PRP gel may provide a beneficial environment, promoting good quality of cartilage repair and upregulating the synthetic capacity of chondrocytes through the growth factor potential. Further, leucocyte inclusion is beneficial due to their role in tissue remodelling and their increased antibacterial and immunological resistance.<sup>33</sup>

Many studies confirmed that PDGF and TGF- $\beta$ 1 help chondrocytes to maintain the hyaline-like chondrogenic phenotype and induce the proliferation and deposition of cartilage matrix molecules such as type II collagen and proteoglycan.<sup>25,34</sup> A recent study reported that the histological evaluation of an osteochondral lesion treated with PRP over 180 days exhibited superior results for the PRP group, compared to the untreated group.<sup>35</sup> These results are in line with the findings of our study, which present good histological results (cell morphology, surface regularity, chondral thickness, and repair tissue integration) for the PRP-treated groups compared to the controls.

Milano et al<sup>36</sup> reported improved gross and histological findings, as well as an increased type II collagen deposition, when using PRP as an adjunct to microfracture surgery for osteochondral lesions. Similar results have been described when PRP was combined with poly(lactide-co-glycolic acid) (PLGA) scaffold,<sup>1</sup> collagen matrix,<sup>37</sup> or autologous osteochondral graft.<sup>24</sup>

However, not all studies reported favourable outcomes as a result of PRP administration. In a sheep model,<sup>26</sup> PRP gel was used to assess the regeneration of the osteochondral defects in sheep knee cartilage. The results indicated that PRP had reparative properties, but mostly by stimulating the formation of fibrocartilaginous tissue, in addition to the recent study that evaluated the effect of PRP gel and PRP in PLGA carrier. After weeks 4 and 12, PRP gel and PRP + PLGA groups showed fibrous and fibrocartilaginous tissue, with higher expressions of COL I, TNF- $\alpha$ , interleukin-6 (IL-6), and matrix metalloproteinase-3 (MMP-3).<sup>38</sup> Our results indicate exactly the opposite, with a high index of cartilage reparation inside the defect of the treated groups, as well as an increased type II collagen expression at week 3, which was enhanced at week 12.

Some studies support and others refute the capacity of PRP gel to regenerate the osteochondral cartilage defect with a good quality of the neoformed tissue. These contrasts may be explained by the interactions of the endogenous synthesis of PRP and the adjuncts when

combined. In addition, the lack of a standard method of PRP preparation includes the laboratory conditions, the cytological component of PRP, and the tolerance and the physiological reaction of each animal to PRP. In that regard, several attempts have been made to characterize and classify PRP but no consensus has been reached. However, a standardized universal nomenclature as well as a comprehensive and reproducible classification system for autologous blood-derived products remains necessary.<sup>39</sup>

In conclusion, our results indicate that the use of PRP gel without adjunct can regenerate the osteochondral full-thickness defects in the femoral trochlea of a rabbit model. The macroscopic and histological results at week 12 were similar to one another, thus demonstrating a normal characteristic of hyaline cartilage-like tissue.

### Supplementary material



ARRIVE checklist, showing that the authors adhered to the ARRIVE guidelines in this study.

### References

1. Sun Y, Feng Y, Zhang CQ, Chen SB, Cheng XG. The regenerative effect of platelet-rich plasma on healing in large osteochondral defects. *Int Orthop*. 2010;34(4):589–597.
2. Buckwalter JA, Mankin HJ. Articular cartilage repair and transplantation. *Arthritis Rheum*. 1998;41(8):1331–1342.
3. Craig W, David JW, Ming HZ. A current review on the biology and treatment of the articular cartilage defects (part I & part II). *J Musculoskelet Res*. 2003;7:157–181.
4. Getgood A, Brooks R, Fortier L, Rushton N. Articular cartilage tissue engineering: today's research. tomorrow's practice? *J Bone Joint Surg Br*. 2009;91-B:565–576.
5. Panseri S, Russo A, Cunha C, et al. Osteochondral tissue engineering approaches for articular cartilage and subchondral bone regeneration. *Knee Surg Sports Traumatol Arthrosc*. 2012;20(6):1182–1191.
6. Rodeo SA. Cell therapy in orthopaedics: where are we in 2019? *Bone Joint J*. 2019;101-B(4):361–364.
7. Xie X, Wang Y, Zhao C, et al. Comparative evaluation of MscS from bone marrow and adipose tissue seeded in PRP-derived scaffold for cartilage regeneration. *Biomaterials*. 2012;33(29):7008–7018.
8. Alsousou J, Thompson M, Hulley P, Noble A, Willett K. The biology of platelet-rich plasma and its application in trauma and orthopaedic surgery: a review of the literature. *J Bone Joint Surg Br*. 2009;91-B(8):987–996.
9. King SM, Reed GL. Development of platelet secretory granules. *Semin Cell Dev Biol*. 2002;13(4):293–302.
10. Akeda K, An HS, Okuma M, et al. Platelet-Rich plasma stimulates porcine articular chondrocyte proliferation and matrix biosynthesis. *Osteoarthritis Cartilage*. 2006;14(12):1272–1280.
11. Park S-I, Lee H-R, Kim S, Ahn M-W, Do SH, Do Hee S. Time-sequential modulation in expression of growth factors from platelet-rich plasma (PrP) on the chondrocyte cultures. *Mol Cell Biochem*. 2012;361(1-2):9–17.
12. Fukaya M, Ito A. A new economic method for preparing platelet-rich plasma. *Plast Reconstr Surg Glob Open*. 2014;2(6):e162.
13. Freymiller EG, Aghaloo TL. Platelet-Rich plasma: ready or not? *J Oral Maxillofac Surg*. 2004;62(4):484–488.
14. Arora NS, Ramanayake T, Ren Y-F, Romanos GE. Platelet-Rich plasma: a literature review. *Implant Dent*. 2009;18(4):303–310.
15. van den Borne MPJ, Raijmakers NJH, Vanlauwe J, et al. International Cartilage Repair Society (ICRS) and Oswestry macroscopic cartilage evaluation scores validated for use in Autologous Chondrocyte Implantation (ACI) and microfracture. *Osteoarthritis Cartilage*. 2007;15(12):1397–1402.
16. Ronga M, Angeretti G, Ferraro S, DE Falco G, Genovese EA, Cherubino P. Imaging of articular cartilage: current concepts. *Joints*. 2014;2(3):137–140.
17. Goebel L, Zurakowski D, Müller A, Pape D, Cucchiari M, Madry H. 2D and 3D MOCART scoring systems assessed by 9.4 T high-field MRI correlate with

- elementary and complex histological scoring systems in a translational model of osteochondral repair. *Osteoarthritis Cartilage*. 2014;22(10):1386–1395.
18. Schmitz N, Laverty S, Kraus VB, Aigner T. Basic methods in histopathology of joint tissues. *Osteoarthritis Cartilage*. 2010;18 Suppl 3:S113–S116.
  19. Mainil-Varlet P, Aigner T, Brittberg M, et al. Histological assessment of cartilage repair: a report by the histology endpoint Committee of the International cartilage repair Society (ICRS). *J Bone Joint Surg Am*. 2003;85-A Suppl 2:45–57.
  20. Hoemann C, Kandel R, Roberts S, et al. International Cartilage Repair Society (ICRS) Recommended Guidelines for Histological Endpoints for Cartilage Repair Studies in Animal Models and Clinical Trials. *Cartilage*. 2011;2(2):153–172.
  21. Wayne JS, McDowell CL, Shields KJ, Tuan RS. In vivo response of poly(lactic acid)-alginate scaffolds and bone marrow-derived cells for cartilage tissue engineering. *Tissue Eng*. 2005;11(5-6):953–963.
  22. Marmotti A, Rossi R, Castoldi F, Roveda E, Michielon G, Peretti GM. Prp and articular cartilage: a clinical update. *Biomed Res Int*. 2015;2015:1–19.
  23. Alsousou J, Ali A, Willett K, Harrison P. The role of platelet-rich plasma in tissue regeneration. *Platelets*. 2013;24(3):173–182.
  24. Smyth NA, Murawski CD, Fortier LA, Cole BJ, Kennedy JG. Platelet-Rich plasma in the pathologic processes of cartilage: review of basic science evidence. *Arthroscopy*. 2013;29(8):1399–1409.
  25. Lee J-C, Min HJ, Park HJ, Lee S, Seong SC, Lee MC. Synovial membrane-derived mesenchymal stem cells supported by platelet-rich plasma can repair osteochondral defects in a rabbit model. *Arthroscopy*. 2013;29(6):1034–1046.
  26. Carneiro MdeO, Barbieri CH, Barbieri Neto J, Neto JB. Platelet-Rich plasma gel promotes regeneration of articular cartilage in knees of sheeps. *Acta Ortop Bras*. 2013;21(2):80–86.
  27. Weibrich G, Hansen T, Kleis W, Buch R, Hitzler WE. Effect of platelet concentration in platelet-rich plasma on peri-implant bone regeneration. *Bone*. 2004;34(4):665–671.
  28. Parrish WR, Roides B. Physiology of blood components in wound healing: an appreciation of cellular co-operativity in platelet rich plasma action. *JESD*. 2017;4(2):1–14.
  29. Zhao R, Wang S, Jia L, Li Q, Qiao J, Peng X. Interleukin-1 receptor antagonist protein (IL-1ra) and miR-140 overexpression via pNNS-conjugated chitosan-mediated gene transfer enhances the repair of full-thickness cartilage defects in a rabbit model. *Bone Joint Res*. 2019;8(3):165–178.
  30. Qi YY, Chen X, Jiang YZ, et al. Local delivery of autologous platelet in collagen matrix simulated in situ articular cartilage repair. *Cell Transplant*. 2009;18(10):1161–1169.
  31. Alford JW, Cole BJ. Cartilage restoration, part 1: basic science, historical perspective, patient evaluation, and treatment options. *Am J Sports Med*. 2005;33(2):295–306.
  32. Smith GD, Knutsen G, Richardson JB. A clinical review of cartilage repair techniques. *J Bone Joint Surg Br*. 2005;87(4):445–449.
  33. Bart WO, Joost CP. Rianne H in 't Veld, Anne JHV. Concentrations of Blood Components in Commercial Platelet-Rich Plasma Separation Systems A Review of the Literature. *Am J Sport Med*. 2018:1–8.
  34. Schmidt MB, Chen EH, Lynch SE. A review of the effects of insulin-like growth factor and platelet derived growth factor on in vivo cartilage healing and repair. *Osteoarthritis Cartilage*. 2006;14(5):403–412.
  35. Danieli MV, Pereira HdaR, Carneiro CAdeS, Felisbino SL, Deffune E. Treatment of osteochondral injuries with platelet gel. *Clinics*. 2014;69(10):694–698.
  36. Milano G, Sanna Passino E, Deriu L, et al. The effect of platelet rich plasma combined with microfractures on the treatment of chondral defects: an experimental study in a sheep model. *Osteoarthritis and Cartilage*. 2010;18(7):971–980.
  37. Wu C-C, Chen W-H, Zao B, et al. Regenerative potentials of platelet-rich plasma enhanced by collagen in retrieving pro-inflammatory cytokine-inhibited chondrogenesis. *Biomaterials*. 2011;32(25):5847–5854.
  38. Chang N-J, Erdenekhyag Y, Chou P-H, Chu C-J, Lin C-C, Shie M-Y. Therapeutic effects of the addition of platelet-rich plasma to Bioimplants and early rehabilitation exercise on articular cartilage repair. *Am J Sports Med*. 2018;46(9):2232–2241.
  39. Rossi LA, Murray IR, Chu CR, Muschler GF, Rodeo SA, Piuze NS. Classification systems for platelet-rich plasma. *Bone Joint J*. 2019;101-B(8):891–896.

#### Author information:

- F. Slimi, MSc, PhD, Research Fellow
- W. Zribi, MD, Professor, Orthopaedic Surgeon
- M. Trigui, MD, Professor, Orthopaedic Surgeon
- R. Amri, MSc, PhD, PhD Student
- M. A. Rebai, MD, Orthopaedic Surgeon
- H. Keskes, MD, Professor, Orthopaedic Surgeon  
Experimental Surgery of the Musculoskeletal System Laboratory, Faculty of Medicine, Sfax, Tunisia.
- N. Gouiaa, PhD, University Hospital Professor, Pathologist
- T. Boudawara, MD, Professor, Anatomopathologist  
Department of Pathology, Habib Bourguiba Hospital, Sfax, Tunisia.
- C. Abid, MSc, Research Fellow, Laboratory of Molecular and Cellular Screening Processes (LPCMC), Biotech Center of Sfax, Sfax, Tunisia.
- S. Jebahi, PhD, Associate Professor, Laboratory of Molecular and Cellular Screening Processes (LPCMC), Biotech Center of Sfax, Sfax, Tunisia; Energy and Matter Research Laboratory, National Center for Nuclear Science and Technology (CNSTN), Sidi Thabet, Tunisia.

#### Author contributions:

- F. Slimi: Conducted the experiments, Collected and analyzed the data, Prepared the manuscript.
- W. Zribi: Edited the manuscript.
- M. Trigui: Evaluated the MRI scans, Operated on the animals.
- R. Amri: Handled the histological protocol.
- N. Gouiaa: Evaluated the histological analysis.
- C. Abid: Conducted the statistical analysis.
- M. A. Rebai: Evaluated the MRI scans.
- T. Boudawara: Conducted the histological evaluation.
- S. Jebahi: Edited the manuscript.
- H. Keskes: Supervised the work.

#### Funding statement:

- No benefits in any form have been received or will be received from a commercial party related directly or indirectly to the subject of this article.

#### Ethical review statement:

- All surgical procedures and care for rabbits were approved by the Animal Research Ethics Committee of our university, in compliance with the internationally recognized principles for the care and use of laboratory animals, and judged commendable by the Committee of Animal Ethics (Protocol no. 94–1939).

© 2021 Author(s) et al. This is an open-access article distributed under the terms of the Creative Commons Attribution Non-Commercial No Derivatives (CC BY-NC-ND 4.0) licence, which permits the copying and redistribution of the work only, and provided the original author and source are credited. See <https://creativecommons.org/licenses/by-nc-nd/4.0/>.